Int. Journal of Vehicle Design, Vol. X, No. Y, 2005

Large-Eddy Simulation for the Prediction of Aerodynamics in IC Engines

L. Thobois*, G. Rymer⋆, T. Soulères⋆⋆, T. Poinsot† and B. Van den Heuvel‡

* CFD Team, CERFACS, 42 - Avenue Gaspard Coriolis, 31057 Toulouse Cedex 01, France, thobois@cerfacs.fr

⋆ Research Department, PSA Peugeot Citroën, 8 - Route de Gisy, 78943 Vélizy, France, guillaume.rymer@mpsa.com

⋆⋆ Research Department, PSA Peugeot Citroën, 18 - Rue des Fauvelles, 92256 La Garenne-Colombes Cedex, France, thierry.souleres@mpsa.com

† EEC Group, IMF Toulouse, 1 - Allée du Professeur Camille Soula, 31400 Toulouse, France, thierry.poinsot@imft.fr

‡ FORD Research Centre Aachen, Suesterfeldstrasse 200, D-52072, Aachen, Germany, svanden5@ford.com

Abstract: In this paper, large-eddy simulation techniques are used to predict aerodynamics through diesel engine intake ports under steady-flow conditions. For the first test case, swirling flows are investigated through an axisymmetric sudden expansion. The LES swirl profile predicted is compared with experimental measurements. For the second test case, a sudden expansion with a valve is tested, where discharge coefficient is compared to experimental data. For the third test case, the same approach is applied to a real engine geometry which has two intake ports. Both the swirl profile and the discharge coefficient are calculated and compared to experiments.

Keywords: Large-Eddy Simulation, dielse engines, intake ports, aerodynamics, steady state flow bench, swirl flows, valve, pressure loss, discharge coefficient, swirl.

Reference to this paper should be made as follows: Thobois L., Rymer G., Soulères T., Poinsot T. and Van den Heuvel B., Large-Eddy Simulation for the Prediction of Aerodynamics in IC engines., Int. J. Vehicle Design, *"New strategies in Automotive Diesel Engines for Meeting Upcoming Pollutant Emission Restrictions"*,2005

Nomenclature

Abbr.	Unit	Definition
A_R	m^2	Reference area based on the inner seat diameter
c	$m.s^{-1}$	Sound speed
C_D	-	Discharge coefficient
ΔP	Pa	Pressure loss
p_0	Pa	Upstream stagnation pressure
p_T	Pa	Total pressure

$\dot{m}$	$kg.s^{-1}$	Mass flow rate
R_g	$Pa.kg^{-1}.m^{-3}.K^{-1}$	Perfect gas constant
Re	-	Reynolds number
S	-	Swirl number
T_0	K	Upstream stagnation temperature
T_{CPU}	$[h.\tau_c^{-1}]$	CPU time on a SGI Origin 3800
u	$m.s^{-1}$	Mean axial velocity
u_{bulk}	$m.s^{-1}$	Rating velocity at the inlet
$\vec{u}$	$m.s^{-1}$	Local velocity vector
w	$m.s^{-1}$	Mean tangential velocity
x_{min}	mm	Smallest cell dimension of the domain
$y+$	-	Non dimensionalized wall coordinate
γ	-	Heat capacity ratio
ρ	$kg.m^{-3}$	Density
τ_{av}	s	Averaging time

1 Introduction

The development of diesel engines consists of the optimization of many parameters, such as pollutant emissions, consumption and durability. In this context, CFD is a powerful tool for design engineers supplementary to experiments. On one hand, the 3D fields of the computed variables can be analysed and used to better understand the physical phenomena taking place. On the other hand, the optimisation of geometrical details can be carried out more easily numerically than experimentally. During the last decades, numerous computational studies have been achieved in IC engines using the RANS approach equipped with a k-ϵ model or a RNG model [1][2][3]. Moreover, with the growing of the computational power [4], the large-eddy approach becomes now feasible in complex geometries [5][6][7]. The interest for LES comes from the flow pattern in internal combustion engines. The flow is very turbulent with small dissipative structures but contains also some main large structures. For instance, in diesel engines, a swirl motion is initiated by the bended intake ports. LES will be able to resolve these structures and give better results than RANS computations.

Phenomena taking place in internal combustion engines depend on these main structures. They are also more and more important in regards to the new combustion concepts, based on direct injection for example. The typical way to study the aerodynamics of IC geometries is to transform them in a steady state flow bench problem [8][9][10]. Piston and exhaust valves are put out. The airflow passes though the intake port(s), enters into the cylinder, which is directly linked to the outlet.

In this study, LES is compared to experiments in three steady state flow benches. First, a swirling flow is tested through a sudden expansion. The swirl profile obtained along the configuration is compared to the swirl profile calculated from the LDA measurements. Secondly, a sudden expansion with one valve is tested. LES axial velocities profiles are compared to LDA measurements and to RANS computations. Moreover, the static pressure axial profile and the characteristic discharge coefficient are compared to experimental measurements. Finally, a geometry with two real bended intake ports is investigated. The axial and tangential mean velocities are compared to DGV experiments and RANS computations. The swirl profile is then compared to experiments and RANS, as well as the discharge coefficient.

2 The use of CFD in engine design

The prediction of the discharge coefficient and the swirl number is crucial for the design of diesel intake ports. They are measured or calculated through steady state flow benches. The discharge coefficient allows the evaluation at a specific lift and for a specific engine of the mass flow rate, which can enter the cylinder for a given pressure loss through the bench. It is calculated using eq. 1 [15].

$$C_D = \frac{\dot{m}}{A_R} \frac{\sqrt{R_g T_0}}{p_0} \left(\frac{p_0}{p_T}\right)^{\frac{1}{\gamma}} \left\{ \frac{2\gamma}{\gamma - 1} \left[1 - \left(\frac{p_T}{p_0}\right)^{\frac{\gamma-1}{\gamma}} \right] \right\}^{-\frac{1}{2}} \tag{1}$$

The swirl number is one of the parameters which controls mixing during the intake and compression strokes. It is calculated at a given abscissa x of a configuration from eq. 2 [14]. In this paper, the swirl number is used as a criteria to validate LES results with experimental measurements.

$$S(x) = \frac{1}{R(x)} \frac{\int_0^{R(x)} \int_0^{2\pi} \rho u w r^2 \, d\theta \, dr}{\int_0^{R(x)} \int_0^{2\pi} \rho u^2 r \, d\theta \, dr} \tag{2}$$

Commonly, the characteristic swirl number of a diesel engine is calculated or measured at $x = 1.75$ bore from the cylinder head.

Finally, the Reynolds number is calculated for each configuration from eq. 3.

$$Re = \frac{\rho u D}{\mu} = \frac{\dot{m} D}{S \mu} \tag{3}$$

Where ρ is the fluid density, μ is the fluid dynamical viscosity, D is the diameter of the inlet section and $\dot{m}$ is the mass flow rate.

3 Numerical considerations

The flow solver used is a compressible LES code, called AVBP, developed at Cerfacs. This code is massively parallel thanks to the MPI library. This particular architecture leads to strong flexibility for computations on large meshes using as many processors as required. The code can use either structured and unstructured meshes [21].

Sub-grid scale models The sub-grid scale model used in the present study is a specific one, developed at Cerfacs called, WALE [18]. This sub-grid scale model is a zero-equation closure model. It is based on the Smagorinsky model but does not dissipate small structures near solid boundaries. The model constants used for all the computations in this paper have been set-up for academic configurations such as turbulent channel and homogenous isotropic turbulence.

Numerical methods In AVBP, the discretisation of the governing equations is based on a cell-vertex finite-volume method [11]. A Lax-Wendroff central space differencing is employed. This numerical scheme is used in this study. However, a third order scheme is also present in AVBP. TTGC is based on a Taylor-Galerkin Finite-Element approximation [17].
AVBP is fully explicit. For non-reacting flows, the time step is determined by the minimum of the convective time step. The convective time-step is determined by a Courant-Friedrichs-Lewy number, $CFL \simeq 0.7$:

$$\Delta t_{min} = CFL \, \frac{\Delta x_{min}}{\|\vec{u}\| + c} \tag{4}$$

The temporal integration of the governing equations is handled by a k-stage Runge-Kutta method.

Boundary conditions The compressible Navier-Stokes equations require the use of non-reflecting formulations for the boundary conditions to let waves exit the computational domain. The NSCBC characteristic method is used to impose flow conditions on the inflow and outflow boundaries [20]. No turbulence injection is imposed at the inlet.

Initial solutions In this study, the flow velocity field is set initially to zero, while pressure and temperature are set to the outlet pressure and to the experimental temperature of the fluid respectively. The mass flow rate is progressively increased with a small relaxation coefficient of the characteristic inlet boundary until it reaches the experimental value.

4 Axisymmetric sudden expansion

The first test case is an axisymmetric sudden expansion, simulated with a swirl motion imposed at the inlet. The swirl number is 0.6. This configuration has been investigated experimentally by Dellenback [12]. A database of LDA velocity measurements is available and can be compared to LES results. The computations are performed on a full three-dimensional mesh (Fig. 1), since LES in two dimensions cannot reproduce the right behavior of swirling flows as shown by Schl$\ddot{u}$ter et al. [13][16]. The mesh is structured and is composed of 108000 cells. The maximum of $y+$ is equal to 100 in the whole domain.

The computational domain starts one downtream pipe diameter, D, upstream the expansion, where Dellenback made measurements. It ends fifteen diameters downstream into the dump. The experiments were performed using liquid water. As the CFD code used can only simulate the gazeous phase of fluids, the calculation is performed with nitrogen.

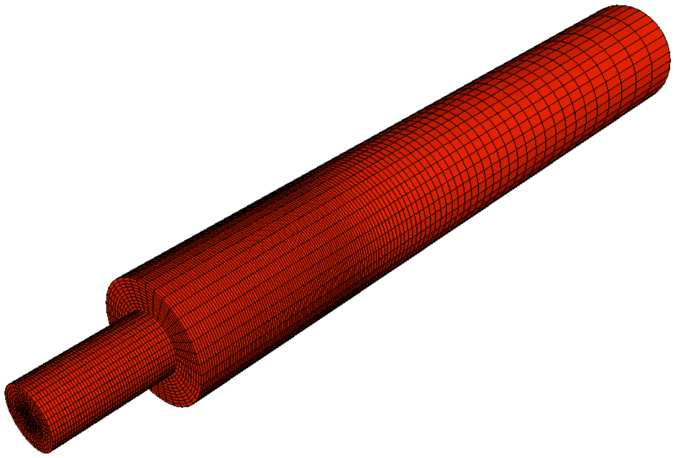

Figure 1: View of the three-dimensional structured mesh of the sudden expansion.

As the effects of compressibility are negligible in this case, the impact of computations with nitrogen is limited. The mass flow rate is chosen to have the same Reynolds number as Dellenback's experiments. No turbulence is injected at the inlet and turbulence develops itself. Solid walls are considered as adiabatic and no slip.

Fluid	N_2
Reynolds number	30000
Mass flow rate, $\dot{m}[kg.s^{-1}]$	0.015
Outlet pressure [Pa]	101300

Table 2: Parameters used for the LES computations

The LES computation lasts in physical time 0.2 s. The instantaneous velocity field is then averaged in time to obtain a mean velocity field and its fluctuations. Fig. 2 compares the LES axial mean and RMS velocity profiles with the LDA profiles at 0.12 x/D from the step. The breakdown of the swirling jet is correctly predicted by LES. The velocity of the central recirculation zone and the velocity of the wall recirculation zone are predicted twice as large by LES. This can explain by the fact that the mesh is not specifically refined at the step. Nevertheless, the level of the axial fluctuations obtained with LES are in good agreement with the measured one, as well as its shape.

The swirl profile along the configuration is presented for LES and LDA in Fig. 3. The bar across the experimental data corresponds to a 20 % error margin. Through the step, the experimental swirl number decreases sharply from 0.6 to 0.3, since radius is doubled at this abscissa in formula 2. After the step, the swirling jet breaks down and the swirl number increases progressively from 0.3 to 0.9. The breakdown of the jet is correctly predicted regarding the swirl increase. Though, LES predicts a swirl drop larger than the measured one at the step. One can notice that in a straight pipe the swirl number decreases very slightly due to the wall friction. The same observations can be made about swirl calculated with LES. There is globally good agreement between the LES results and the LDA measurements except at the end of the configuration. The differences observed at the end of the pipe may come from the progressive coarsening of the mesh.

At 1.75 bore, the swirl predicted by LES is equal to 0.94, whereas the LDA swirl is 0.84,

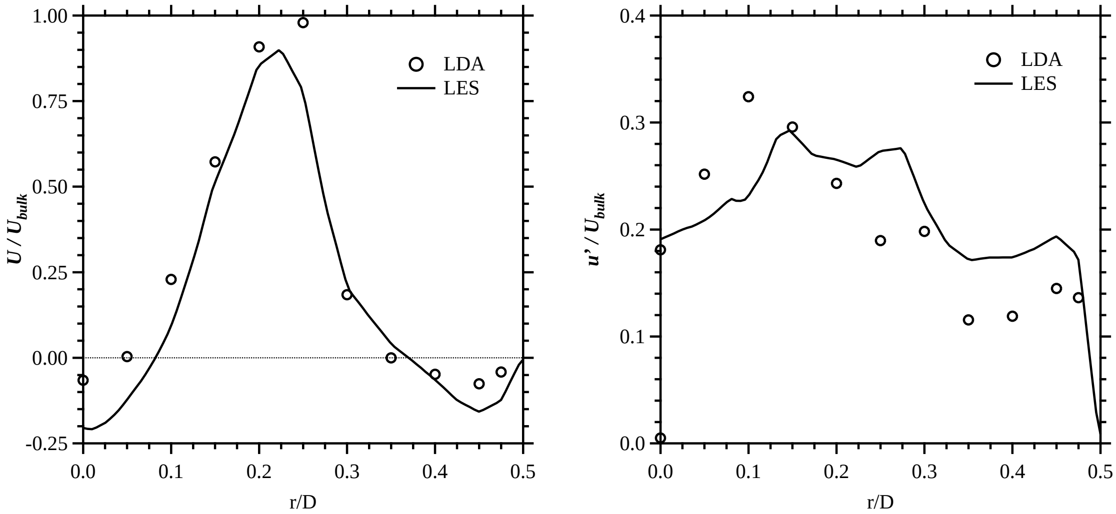

Figure 2: Comparison of the swirl profile obtained with LES and LDA at 0.12 x/D from the step.

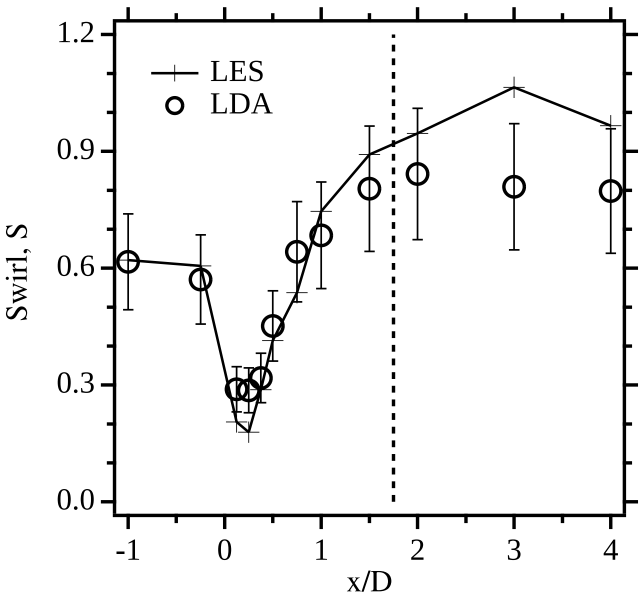

Figure 3: Comparison of the swirl profile obtained with LES and LDA.

leading to an error of 10 % in the swirl prediction.

5 Axisymmetric sudden expansion with a valve

The second configuration consists of an axisymmetric sudden expansion with a valve. The diameter of the upstream pipe is multiplied by 3.5 through the step. The diameter of the downstream pipe is called D in this section. LDA measurements are available [19], as well as RANS computations [1]. RANS computations are performed with KIVA and the standard $k-\epsilon$ turbulence model [24]. The 3D structured mesh is composed of 125000 cells to limit the CPU time. As the resolution near walls is limited (the mean of y+ is equal to 300), wall function is used to calculate the wall stress and to set the near-wall node velocities [25][26].

The LES computations are performed on a full three-dimensional structured mesh, composed of 400000 cells, as shown in Fig. 4. The mesh consists of a H-type mesh. The region near the valve is refined. The cell size is progressively increased towards the outermost left (inlet) and the outermost right (outlet). The maximum $y+$ is equal to 100 at the valve seat and at the valve head.

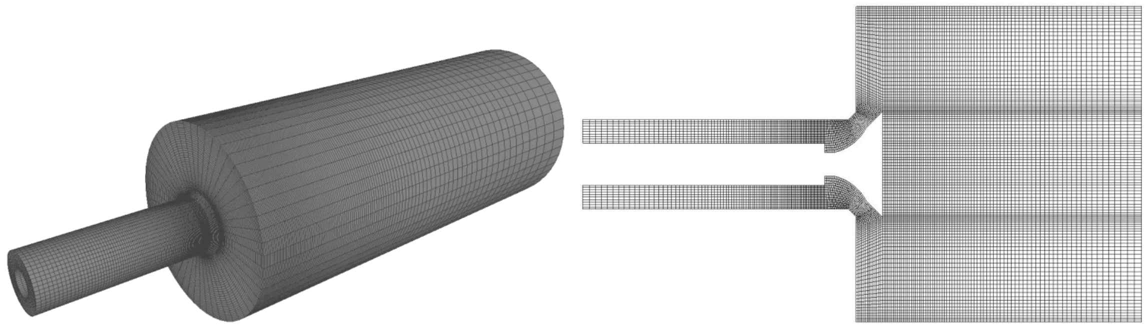

Figure 4: Views of the three-dimensional mesh.

The inlet profile imposed at the inlet is a flat profile. Again, as with the Dellenback's configuration, the mass flow rate is chosen to have the same Reynolds number as the experiments. Solid walls are considered as adiabatic and no slip.

Fluid	N_2
Reynolds number	30000
Mass flow rate, $\dot{m}[kg.s^{-1}]$	0.015
Outlet pressure [Pa]	101300

Table 3: Parameters used for the LES computation.

Fig. 5 shows the profiles of the axial mean velocity and its fluctuation at 0.33 x/D from the cylinder head. LES results are compared with the LDA measurements and with the RANS computations. There is a good agreement between LES and LDA. The peaks due to the breakdown of the valve jet is better predicted by LES than by RANS. Significantly, the sharp peaks of fluctuations are well captured by LES, while the RANS computations capture approximatively the location of these peaks, and hardly reproduce the fluctuations of the peaks, which are smaller by half than the experimental ones. The over-prediction of fluctuations near walls with LES comes from the WALE model, which puts almost zero viscosity near walls.

The static pressure profile obtained with LES is compared to the experimental data in Fig. 6. The global pressure loss through the configuration predicted by LES is equal to 1730 Pa, whereas the measured result is of 1910 Pa. The error is then equal to 9 %. Both in the experimental and in the LES pressure profiles, four parts can be distinguished. The first part, located at 0 x/D corresponds to the pressure drop induced by the valve. Then, at about 0.75 x/D, the sudden increase comes from the impingement of the valve jet to the wall. The peak reached is correctly predicted. At 1 x/D, the jet rebounds on the

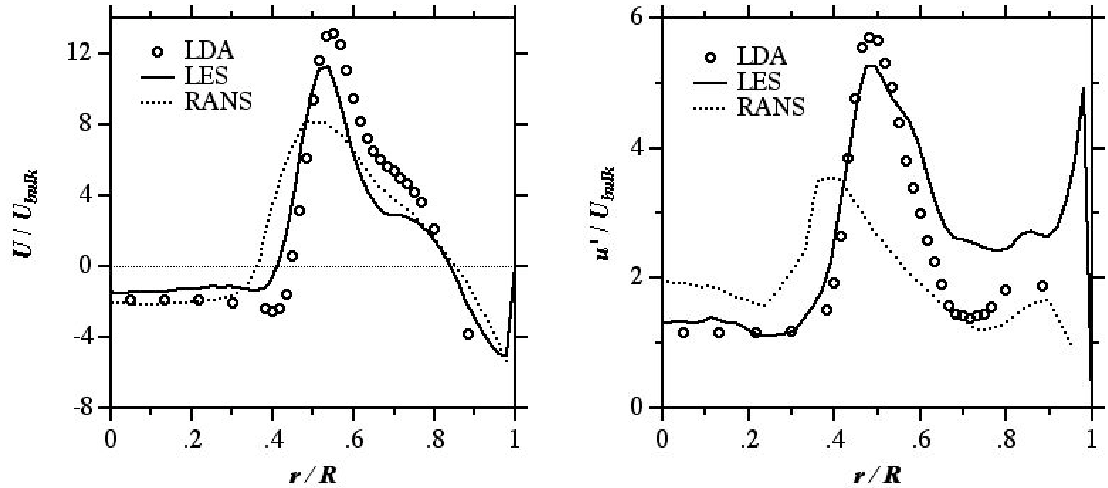

Figure 5: Profiles of the axial mean velocity and its fluctuation at $20mm$ from the cylinder head.

walls, which creates a small depression. Finally, the fourth zone comes from the fluid re-attachement on the wall at 3 x/D. The discharge coefficient has been calculated. The discharge coefficient calculated with LES is 0.175, whereas the experimental discharge coefficient is 0.163. The error is about 7.4 %.

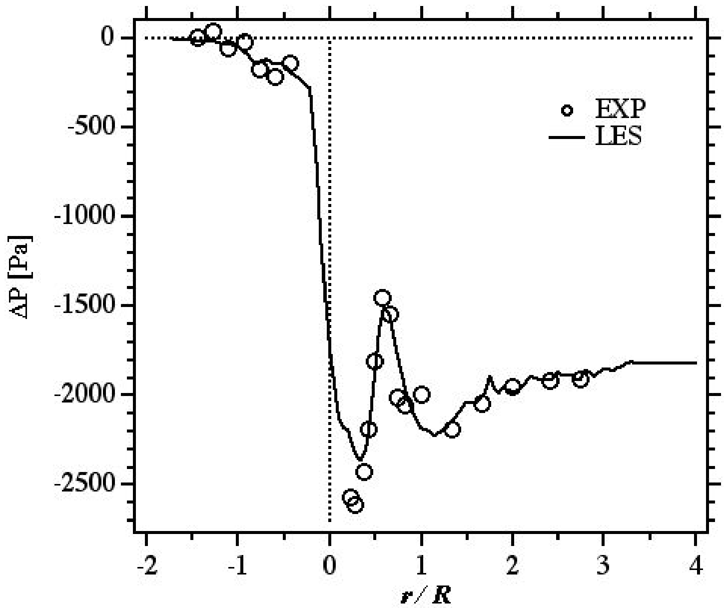

Figure 6: Static pressure profile along the configuration obtained with LES and the experimental measurements.

6 Real engine intake ports

The real geometry is composed of a tank, two bended intake ports, a cylinder and a silencer. One port is tangential, the other one is helical (Fig. 7). The valve lift is 8 mm.

Detailed DGV experiments provide a complete mean velocity database [22]. DGV is an optical measurement technique that allows for rapid acquisition of averaged planar flow field data. RANS computations are performed on an unstructured mesh, composed of about 1.6 millions hexaedra with FIRE V8, the standard $k-\epsilon$ turbulence model and wall laws. In these computations, the pressure difference between the plenum and the silencer is imposed instead of the mass flow rate.

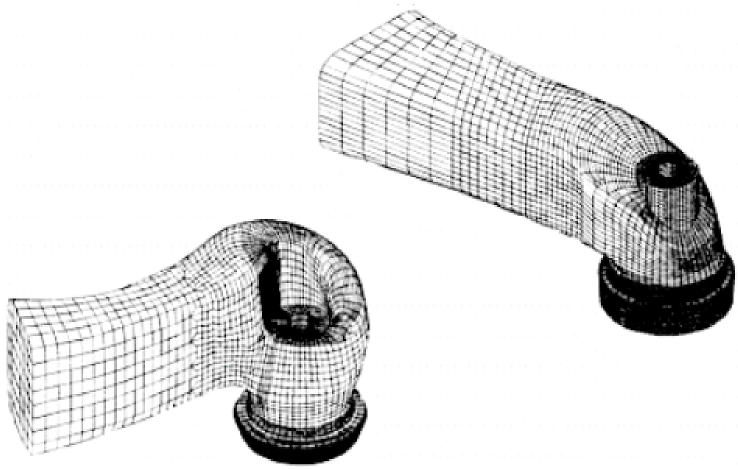

Figure 7: Examples of an helical pipe (left) and a tangential pipe (right) [23].

The unstructured computational mesh used for LES contains 420000 nodes and 2170000 tetraedra. There is no specific refinement near the wall. Though the mesh is refined near the valve stems, the valve heads and the valve seats. This leads to a maximum value of $y+$ of 100 at these locations.
At the inlet a flat profile is imposed and again, the mass flow rate is chosen to have the same Reynolds number as the experiments, that is to say $Re \simeq 80000$. Again, solid walls are considered as adiabatic and no slip.

Fig. 8 and 9 represent the axial and tangential mean velocity fields obtained with the LES and RANS computations and the DGV measurements at 0.12 D from the cylinder head, where D is the bore of the cylinder. On these figures, the tangential port is located at the upper half and the helical port at the downer half. The maxima of axial velocity represent the valve jets and the minima represent the recirculation downstream the cylinder head and the valve heads. RANS predicts a little bit better the breakdown of the tangential jet than LES, whereas LES predicts better the breakdown of the helical jet. This can be explained by the fact that the mesh used for the RANS computations is clearly better refined near the valve seats than the mesh used for the LES computations. As the flow in the tangential port is more separated than the flow in the helical one, RANS can better predict the flow fields near the tangential port. In looking at the tangential velocity fields, LES is in better agreement with DGV than RANS.

Fig. 10 and 11 represent the axial and tangential mean velocity fields obtained with the LES and the RANS computations and the DGV measurements at 1.75 D from the cylinder head. One can first note the asymmetry of the 2D fields both for the axial and tangential mean velocities. At this location, the two valve jets can be no more distinguished. The flow consists of a solid body rotation thrown off centre. It is important to observe that LES is able to predict with a good agreement the position and the intensity of the extrema,

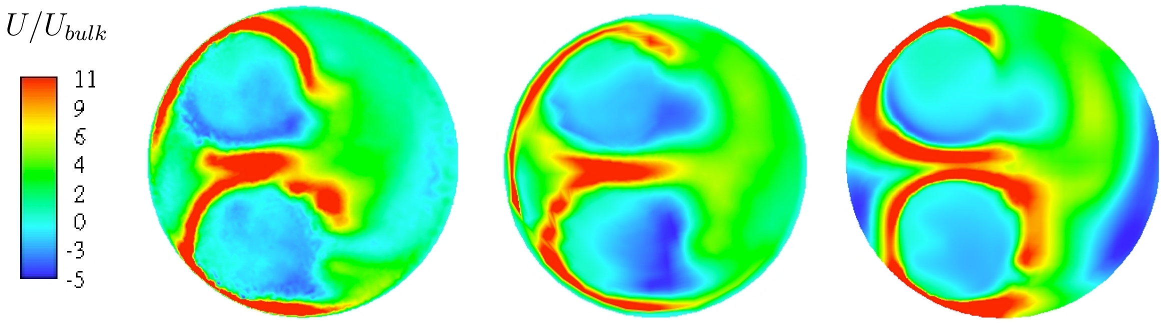

(a) LES (b) DGV (c) RANS

Figure 8: Axial mean velocity fields U at 0.12 D from the cylinder head.

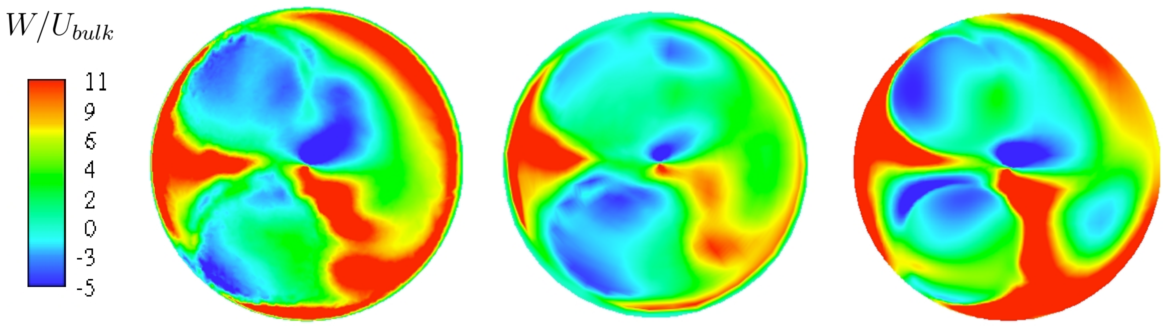

(a) LES (b) DGV (c) RANS

Figure 9: Tangential mean velocity fields W at 0.12 D from the cylinder head.

whereas RANS does not in this particular case.

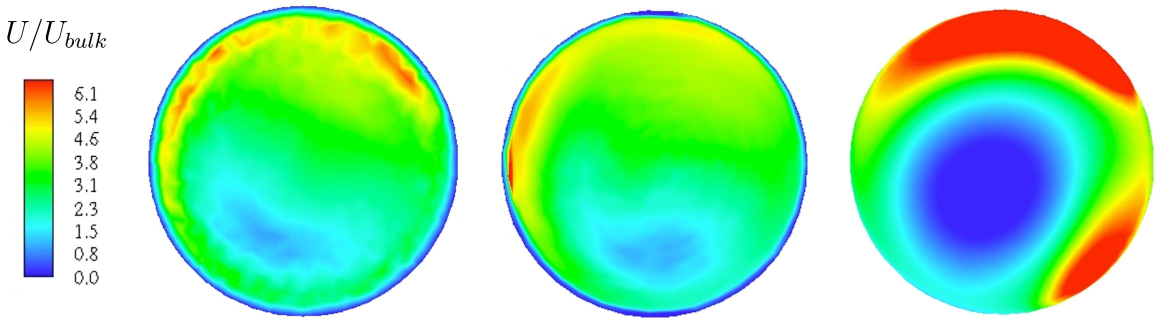

(a) LES (b) DGV (c) RANS

Figure 10: Axial mean velocity fields U at 1.75 D from the cylinder head.

More quantitatively, the LES and RANS swirl profiles are compared to the experimental data, as shown in Fig. 12. The bar across the experimental data corresponds to a 10 % error margin. The swirl increases throughout the cylinder since the two valve jets join that is to say until one diameter. After one diameter, the wall friction phenomena become preponderant and the swirl decreases. At 0.75 D, the flow is characterized by a solid body rotation. Then, the swirl decreases slightly due to the wall friction. These variations of swirl are well predicted by LES. Nevertheless, one can notice that LES over-estimates the swirl number throughout the configuration and that at the end of the cylinder the swirl decrease is faster. The RANS swirl profile is very different from the experimental

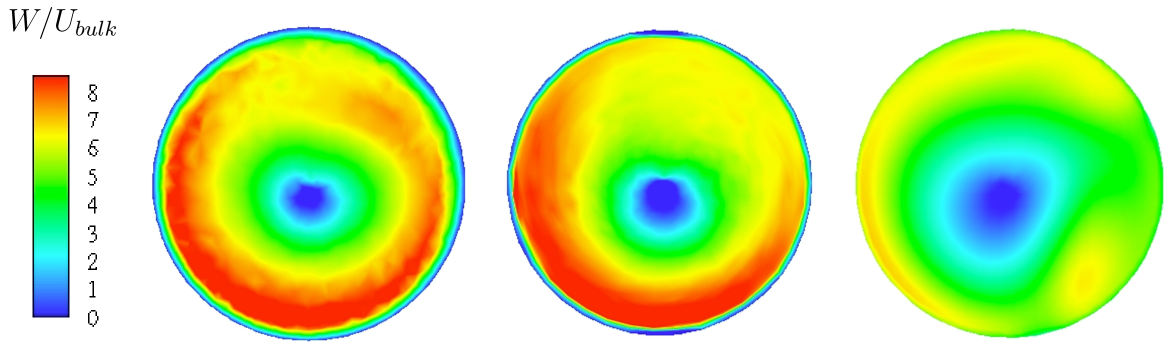

(a) LES (b) DGV (c) RANS

Figure 11: Tangential mean velocity fields W at 1.75 D from the cylinder head.

measurements. The swirl increase is not really captured and at 0.4 D, RANS predicts a swirl almost constant throughout the cylinder.

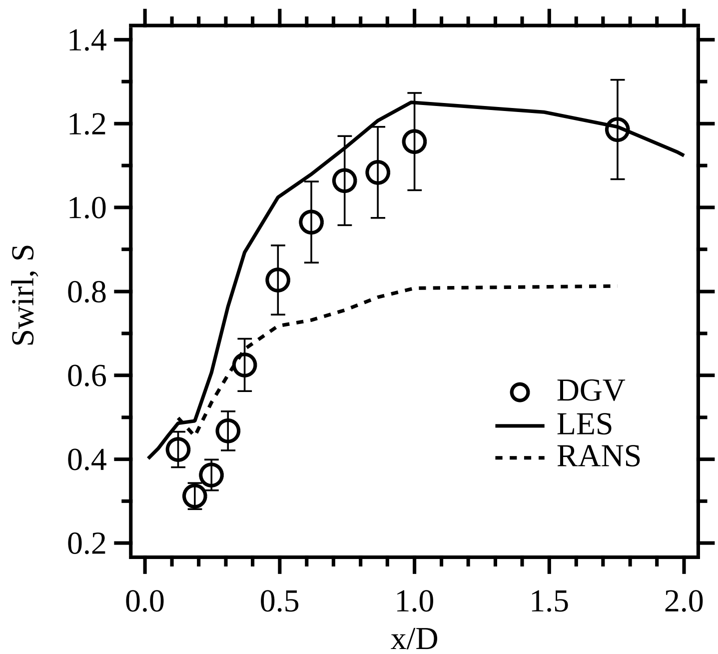

Figure 12: Comparison of the swirl profiles obtained with LES, RANS and DGV.

The swirl and the discharge coefficient are predicted respectively with an error of 1.01 % and 0.85 % with LES. LES shows in this case a particular potential of prediction since no adjustement to the model constants has been undertaken and since the RANS computations predict the swirl with an error of 31.1 % and the discharge coefficient with an error of 13.22 %. The errors made by the RANS computations are highly linked with the over-estimation of the mass flow rate, since only the difference of pressure between the inlet and the outlet is imposed.

7 Conclusion

Table 4 summarises the prediction error in % of LES for swirl and discharge coefficient for the three geometries tested. As well as, the averaging time, τ_{av} and the CPU time, T_{CPU} required to perform one τ_{av} on a SGI Origin 3800 on 64 processors is given. For the real geometry, the LES computation of one τ_{av} takes 100 hours.

Geometry	τ_{av} $[ms]$	T_{CPU} $[h.\tau_{av}^{-1}]$	ΔS	ΔC_D
1	200	1.3	10 %	-
2	20	66.6	-	7.4 %
3	40	100	1.01 %	0.85 %

Table 4: Averaging time, CPU time and prediction error in % of LES for swirl number and discharge coefficient for the three IC geometries tested.

In this paper, LES of three steady state flow benches have been performed. The problem of the numerical calculation of diesel engines has been divided into smaller problems. The quantitative evaluation of the potentiality of LES for each specific phenomena has been realized.
For the first test case, an axisymmetric sudden expansion has been simulated with a swirling flow. The swirl profile predicted by LES has been compared to the one calculated from the LDA measurements. The jet breakdown is correctly captured. The swirl number at 1.75 bore from the step is well predicted with an error of 10 %.
For the second test case, an axisymmetric sudden expansion with a valve has been computed with a non-swirling flow. The comparisons of the axial mean and RMS velocities between LES and LDA show good agreements. Additionally, the discharge coefficient is calculated for the LES results and the experimental data. This comparison exhibits a difference of only 7 %.
Finally, a real geometry with two real bended diesel intake ports has been computed with the LES approach at high lift. This particular case is a critical case difficult to reproduce via the classical RANS approach, that is why it has been chosen as a test case for LES. The comparison of the swirl number between LES, RANS and DGV shows that LES is able to predict a swirl with an error of 1 %, whereas RANS predicts it with an error of 31 %. In addition, the discharge coefficient is predicted by LES with an error of 1 %, whereas with RANS it is predicted with an error of 13 %. The LES 2D velocity fields are qualitatively similar to the one obtained experimentally with the DGV technique. The LES simulation shows here therefore potential as a predictive tool for design purpose.

The presented LES computations are a first step to evaluating the potential of LES in real IC geometries. The next step will be to use the LES techniques in real engines with moving valves and moving pistons to predict the cycle-to-cycle variations.

8 References

1. Lebrère L., "Modélisation de la Turbulence au Second Ordre pour la Simulation Numérique d'Ecoulements dans les Moteurs à Piston", Phd Thesis, Ecole Centrale Lyon

(ECL), 1995.
2. Tahry, E. S. H., "Application of a Reynolds Stress Model to Engine Flow Calculations", J. Fluids Engineering, 107, 444-450, 1985.
3. Payri, S. E., "CFD Modelling of the In-Cylinder Flow in DI Diesel Engines", Computers & Fluids, 33,pp. 995-1021, 2004.
4. Moore, G. E., "Cramming more components onto integrated circuits", Electronics, Volume 38, Number 8, 1965 (19 April)
5. Haworth, D., "Large-Eddy Simulation in In-Cylinder Flows", Oil and Gas Science and Technology, Review IFP, 1999.
6. Verzicco, R., Mohd-Yusof, J., Orlandi, P. and Haworth, D., "LES in Complex Geometries Using Boundary Body Forces", Proceedings of the Summer Program of the Center for Turbulence Research, Stanford University/NASA Ames Center for Turbulence Research, 1998.
7. Yavuz, I., Celik, I., Smirnov, A., "Large-Eddy Simulation of In-Cylinder Turbulence for Internal Combustion Engines : a Review.", Int. J. Engine Research, 2001.
8. Arcoumanis, C., "Internal Combustion Engines - Combustion Treatise", Academic Press, 1988.
9. Winterbone, D.E., Pearson, R.J., "Design Techniques for Engine Manifolds", Professional Engineering Publishing, 1999.
10. Soulères T., "Simulations des Grandes Echelles d'Ecoulements dans des Géometries Fixes et Mobiles : Applications aux Moteurs à Piston", Phd Thesis, Cerfacs, 2003.
11. Schönfeld T., Rudyguard M., "A Cell-vertex Approach to Local Mesh Refinement for the 3d Euler Equations", AIAA papers 1994-0318, 1994.
12. Dellenback P. A., Metzger D. E., Neitzel G. P., "Measurements in Turbulent Swirling Flow Through an Abrupt Axisymmetric Expansion", AIAA journal, Vol. 26, No. 6, June 1988.
13. Schlüter J., Schönfeld T., Poinsot T., Krebs W., Hoffmann S., "Characterization of Confined Swirl Flows using Large Eddy Simulations", The American Society of Mechanical Engineers, 2001-GT-60, 2001.
14. Gupta A. K., Lilley D. G., Syred N., "Swirl Flows", ABACUS Press, Energy and Engineering Science Series, 1984.
15. Heywood J. B., "Internal Combustion Engine Fundamentals", McGraw Hill, 1988.
16. Schlüter J. U., "Large Eddy Simulations of Flow and Mixing in Jets and Swirl Flows: Application to a Gas Turbine", Phd Thesis, Cerfacs, 2000.
17. Colin O., Rudyguard M., "Development of High-Order Taylor-Galerkin Schemes for Unsteady Calculations", Journal of Computationnal Physics, 162(2):338-371,2000.
18. Nicoud, F., Ducros, F., "Subgrid-Scale Stress Modelling based on the Square of the Velocity Gradient Tensor", Flow, Turbulence and Combustion, 62(3): 183-200, 1999.
19. Graftieux L., "Combining LDA and PIV for Turbulence Measurements in Unsteady Swirling Flows", Measurement Science & Technology, vol.12, n9, 2001.
20. Poinsot, T. J., Lele, S. K., "Boundary Conditions for Direct Simulations of Compressible Viscous Reacting Flows", Journal of Computational Physics; CTR Manuscript 102, Centre for Turbulence Research, Stanford, 1992.
21. Schönfeld T., Rudgyard M., "Steady and Unsteady Flow Simulations Using th Hybrid Flow Solver AVBP", AIAA Journal, Vol. 37, No 11, November 1999.
22. Willert, C., Roehle, I., Schodl, R., Dingel, O. and Seidel, T., "Application of Planar Doppler Velocimetry within Piston Engine Cylinders", Proceedings of 11th International Symposium of Laser Techniques to Fluid Mechanics, No. 38-2, 2002.
23. Cyclone Fluid Dynamics, Web site, http://www.cyclone.nl.

24. Amsden, A. A., O'Rourke, P. J. and Butler, T. D., "KIVA II: A Computer Program for Chemically Reactive Flows with Sprays", LA-11560-MS, Los Alamos National Laboratory, Los Alamos, NM, 1989.
25. Buchou, C., "Towards the 3D Modeling of Intake Flow in S.I. Engines Using the Kiva 2 Code", Fourth International Kiva Users Meeting, Detroit, February 1994.
26. Dilies, B. and Fabre, A., "IDI Diesel Engine Combustion Calculations: Influence of the shape of the Prechamber on the Combustion Process", Fifth International Kiva Users Meeting, Detroit, February 1995.

9 Acknowledgements

The authors would like to thank the CINES at Montpellier, France for the CPU hours allocated to this project.
Finally, the authors particularly acknowledge the precious scientific and technical contributions of Olivier Davodet from PSA Peugeot Citroën.

10 Biographical notes

Ludovic Thobois is currently doing a Phd thesis for PSA Peugeot Citroën since 2002. Detached at Cerfacs in the CFD Team, he focuses on the application of large eddy simulation to in-cylinder flows, and especially aerodynamics through diesel engine intake ports under steady-flow conditions. In 2002 he obtained an engineer degree in energy systems.

Guillaume Rymer has been a Technical Specialist for the PSA Peugeot Citroën Research department, Vélizy, France, since 2000. As a member of the Engine CFD simulation team his main focus was on injection and combustion simulation and modeling applied to new gasoline and Diesel engine concept. Since 2003, he has been working in PSA Peugeot Citroën as a project leader. In 1996, he obtained a MSc degree for Fluid Dynamics, Hydraulics engineering and numerical simulations applied to aerodynamics and received his PhD in 2000 for his work on the turbulent combustion modeling.

Thierry Souleres has been a Technical Specialist for the PSA Peugeot Citroën Powertrain design department, La Garenne, France, since 2002. As a member of the combustion system design team his main focus is on CFD simulations for gasoline engine. Between 1999 and 2002 he worked for PSA Peugeot Citroën, detached at Cerfacs (Toulouse, France) in the CFD Team. In 1998 he obtained a MSc degree for Fluid Dynamics and Hydraulics engineering, and received his PhD in 2003 for his work on the application of large eddy simulation approach to in-cylinder flows.

Dr Thierry J. Poinsot received his PhD from Ecole Centrale de Paris in 1983 and his These d'Etat from Universite d'Orsay in 1987. Since 1983, he has been working on reacting flows, first on combustion instabilities, then on numerical combustion. He initiated Direct Numerical Simulation of turbulent flames while at Stanford University in 1988 and has authored more than 150 papers related to turbulent flames, unsteady combustion, active control, direct and large eddy simulation of reacting flows. He is author of the textbook Theoretical and numerical combustion with Pr D. Veynante (R.T. Edwards). Dr Poinsot is a research director at CNRS and the head of the CFD group at CERFACS. He is also a senior scientist at Stanford University and a consultant in many companies and research centers.

Bas van den Heuvel has been a Technical Specialist for the Ford Research Centre Aachen, Germany, since 1999. As a member of the Diesel Research and Advanced Engineering department his main focus is on Diesel combustion system development. Between 1993 and 1999 he was employed at the Engine department of the the Eindhoven University of Technology. In 1993 he obtained a MSc degree for Automotive Engineering, and received his PhD in 1998 for his work on numerical prediction and optical diagnostics of engine aerodynamics.